SPRFMO
South Pacific Regional Fisheries Management Organisation

14th MEETING OF THE SCIENTIFIC COMMITTEE

7 to 12 September 2026, Tórshavn, Faroe Islands

SC14 - DW 12

Improved Particle Dispersal Modelling for Validation of the South Pacific VME Bioregionalisation – Progress Report

New Zealand

South Pacific Regional Fisheries Management Organisation

14th Meeting of the Scientific Committee

Tórshavn, Faroe Islands, 5 September to 12 September 2026

Improved particle dispersal modelling for validation of the South Pacific VME Bioregionalisation – Progress Report

Charine Collins[1], Matthew Bennion[2], Ashley Rowden[1,3], Jennifer Devine[4], Owen Anderson[1], Anthony Charsely[1]

1. Earth Sciences New Zealand, Wellington, New Zealand
2. Earth Sciences New Zealand, Hamilton, New Zealand
3. Victoria University of Wellington, Wellington, New Zealand
4. Earth Sciences New Zealand, Nelson, New Zealand

9 August 2026

Contents

1. Purpose

The purpose of this paper is to update the Scientific Committee on the progress made towards improving the particle dispersal modelling approach used as one validation tool in a multiple-lines-of-evidence approach for the bioregionalisation for Vulnerable Marine Ecosystem (VME) indicator taxa previously reported to the Scientific Committee (SC13-DW10).

2. Background

The Conservation Management Measure (CMM03-2023) for bottom fishing includes a spatial management approach that aims to ensure the long-term conservation and sustainable use of deep-sea fishery resources. The approach protects a large proportion of the predicted distribution of VME indicator taxa (SC11-DW01_rev1), to provide some assurance that bottom fishing within the Evaluated Area would not have Significant Adverse Impacts (SAIs) on vulnerable marine ecosystems (VMEs).

In 2024, New Zealand submitted a paper to the Scientific Committee detailing a bioregionalisation for VME indicator taxa, hereafter referred to as the South Pacific VME Bioregionalisation (SC 12 – DW 11_rev1). However, following its presentation at the 12th Scientific Committee meeting in Lima, Peru, it was agreed that before the bioregionalisation is used (e.g., within impact assessments), that "*further investigations are required to establish whether bioregions may provide an additional spatial scale for evaluating the performance of spatial management measures*" (see sub-task on Multi-annual Work Plan in Annex 4a of COMM13-Report 2025).

Towards addressing this subtask in the Multi-annual Work Plan, validation of the South Pacific VME Bioregionalisation were presented in SC13-DW10. Three approaches were applied as part of a multiple-lines-of-evidence approach methodology to validate the South Pacific VME Bioregionalisation, including validation approaches that draw on independent data (SC13-DW10). The three approaches used were:

> **Approach 1:** Use the same approach as that of Stephenson et al. (2024) to examine classification strength using ANOSIM and to assess the relationship between Bray–Curtis dissimilarity (presence-absence and abundance derived dissimilarity) and distance in transformed environmental space.
>
> **Approach 2**: Use dispersal models (e.g., Lagrangian particle simulation) to assess relative connectivity among bioregions, i.e., relative lack of connectivity between populations of VME indicator taxa.
>
> **Approach 3:** Use independent imagery data to reproduce ANOSIM and similarity percentages (SIMPER) in the same way as carried out in SC 12 – DW 11_rev1 with training data for the South Pacific VME Bioregionalisation.

A key assumption of bioregions is that they represent connectivity, or more accurately, bioregional boundaries represent somewhat porous barriers to connectivity (Klanten et al. 2023). This assumption follows the notion that bioregions represent comparatively unique environmental conditions (Woolley et al. 2019), and communities of species therein, that are distinguishable from other bioregions (Stephenson et al. 2023). Approach 2 was used to test this assumption, using dispersal or particle tracking models (based on hydrodynamics) to assess the level of connectivity (Klanten et al.

2023) for example within, and between, bioregions. The dispersal modelling presented in SC13-DW10 indicated that connectivity between bioregions was generally very low (<5%), whereas connectivity within bioregions was predominantly high (>75%).

The dispersal modelling presented in SC13-DW10 was based on a relatively coarse-resolution (10 km x 10 km grid) global ocean reanalysis product. However, accurately resolving mesoscale eddy dynamics[1] across much of the open ocean generally requires a model with high enough horizontal resolution to resolve, or at least adequately represent, the first baroclinic Rossby radius of deformation (Hallberg et al. 2013). When the horizontal resolution is too coarse, the model's ability to represent baroclinic instabilities[2] and the resulting mesoscale eddy field is reduced, which can affect simulated particle dispersal and connectivity estimates. For the Southwest Pacific region, a horizontal grid spacing of approximately 1-6 km is typically required to resolve mesoscale features such as eddies and fronts (see Figure 12.4 in Le Sommer et al. 2018). Consequently, the dispersal modelling presented at SC 13 (SC13-DW10) is likely to overestimate connectivity within the bioregions while underestimating the between bioregion connectivity.

Furthermore, larval dispersal is governed by the interaction between physical processes operating across a range of spatial and temporal scales and larval life history traits, such as pelagic larval duration, larval mortality and dispersal depth (Cowen and Sponaugle 2009). The latter, which is determined by larval vertical movement in combination with vertical mixing is especially important for deep-sea taxa due to the variations in ocean currents with depth (McVeigh et al. 2017; Gary et al. 2020). McVeigh et al. (2017) and Gary et al. (2020) investigated the influence of larval vertical movement on the dispersal of larvae by simulating a range of possible larval dispersal strategies. The results from both studies demonstrated that the depth of dispersal through vertical movement of larvae significantly altered dispersal pathways and connectivity patterns. Therefore, incorporating biologically realistic larval behaviours, such as vertical movement, is likely to substantially alter the dispersal patterns and connectivity estimates presented in SC13-DW10.

In recognition of the shortcomings of the dispersal modelling presented in SC13-DW10, the Multi-Annual Workplan of the SPRFMO Scientific Committee (COMM14 – Report) includes the following subtask for the Deepwater Working Group:

> Subtask 2.4.3*: To improve the particle tracking model used in the validation of the bioregionalization and investigate connectivity amongst geographically separated areas of the same bioregion.*

To improve upon the dispersal modelling previously undertaken to validate the South Pacific VME Bioregionalisation and address the subtask outlined above, we present preliminary results from particle tracking simulations driven by a high-resolution ocean model of the Southwest Pacific. These simulations incorporate biologically realistic larval behaviours, including depth-dependant drifting and vertical swimming. The following sections of this report describe the high-resolution model, the

[1] Mesoscale eddies, primarily formed through instabilities in ocean currents and fronts, are coherent, rotating features with horizontal scales of approximately 10-100 km in diameter that can persist for weeks to months. They transport heat, salt, nutrients, and biological material, and their formation, evolution, movement, and dissipation collectively (referred to as 'mesoscale eddy dynamics') strongly influence productivity patterns.

[2] Baroclinic instability is the mechanism by which horizontal density gradients and vertical shear in ocean currents become unstable generating the mesoscale eddies that shape species distributions and habitat variability.

different particle tracking simulations and the preliminary results, highlighting how the inclusion of biologically realistic larval behaviours influence dispersal patterns and connectivity.

3. Methods

To improve on the dispersal modelling presented in SC13-DW10, we updated the hydrodynamic model used for the dispersal modelling to a higher-resolution (5 km x 5 km) regional model developed by Earth Sciences New Zealand (ESNZ). In addition, we also investigate the impact of biological behaviour, in particular vertical swimming, on particle dispersal through a number of dispersal scenarios.

Hydrodynamic model of the Southwest Pacific Ocean

Ocean circulation fields for the dispersal modelling were obtained from a high-resolution regional model of the Southwest Pacific Ocean (hereafter referred to as SwPac5). SwPac5 was developed by ESNZ using the Regional Ocean Modelling System (ROMS; Shchepetkin and McWilliams 2005). This model provides physically consistent three-dimensional ocean circulation fields across the Southwest Pacific Ocean, including the New Zealand continental shelf (Figure 3-1). The 5 km horizontal resolution of SwPac5 enables it to resolve large-scale circulation patterns, as well as smaller scale processes such as mesoscale eddies, filaments and fronts. The 50 terrain-following vertical layers (σ-coordinate system), ensures that processes throughout the water column are well represented in the model.

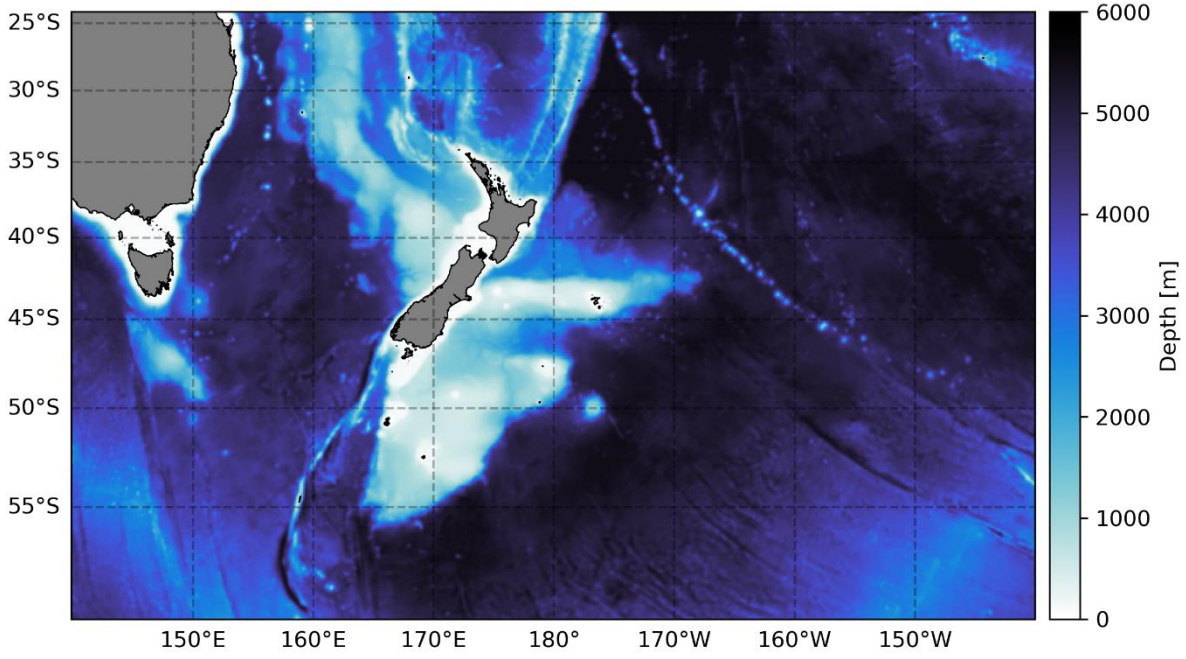

Figure 3-1 | Spatial domain of the SwPac5 ROMS hydrodynamic model, shown with bathymetry (depth in m). The model domain is defined by 1281 x 812 grid cells.

SwPac5 is driven at the ocean surface by wind, heat and freshwater fluxes from the European Centre for Medium-Range Weather Forecasts (ECMWF) ERA-Interim atmospheric reanalysis (Dee et al. 2011). The lateral boundaries of the SwPac5 model domain were forced by oceanic conditions obtained from GLORYS12v1 (Jean-Michel et al. 2021), the global ocean reanalysis product used for the dispersal modelling presented in SC13-DW10.

Lagrangian particle tracking model

The Lagrangian particle tracking model used here is OpenDrift (Dagestad et al. 2018) (found at: https://opendrift.hithub.io/), an open-source offline Lagrangian particle model that can be used to predict the dispersal of particles in the ocean using advection, diffusion, and user-prescribed particle behaviour. Daily velocity fields from SwPac5 were used to compute Lagrangian particle trajectories using a fourth-order Runge-Kutte advection scheme. To account for sub-grid scale hydrodynamic processes not resolved by the hydrodynamic model, a Brownian motion (or random walk) component was included. Following Michie et al. (2024), a horizontal diffusivity coefficient of 0.1176 m^2/s was applied to represent lateral sub-grid scale diffusion. Vertical mixing due to turbulence in the particle tracking model were based on the vertical mixing resolved in SwPac5. Particles remained active for the entire simulation period unless they were advected out of the model domain or encountered the coast, in which case they were considered stranded.

Particle seeding

In all the scenarios (described below), 1,000 particles – representing passive planktonic larvae of VME indicator taxa – were randomly seeded just above the seafloor within each bioregion every week over the course of one year (Figure 3-2). Thus, a total of 53,000 particles were released per bioregion amounting to an overall total of 371,000 particles per scenario. All the scenarios were run for two years to allow all particles to be tracked for a minimum of 365 days.

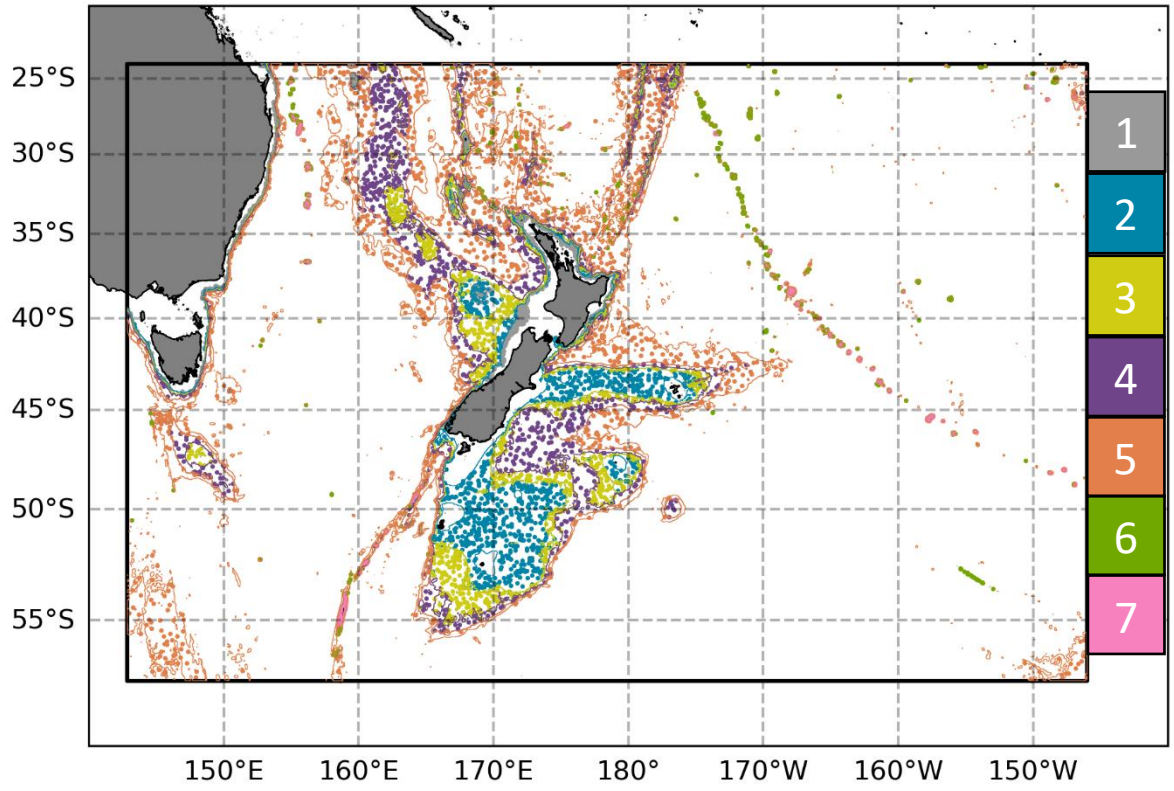

Figure 3-2 | Example of the randomly selected release locations of particles within each bioregion (N = 7). The thin coloured contours indicate the different bioregions colour-coded according to the legend. Particles are also colour-coded according to bioregion. The black rectangular box indicates the boundaries of the study region.

Biological behaviour scenarios

A total of 9 different dispersal scenarios were evaluated. In the first scenario, hereafter referred to as the Control scenario ('Control'), particles are treated as passive tracers, and dispersal is purely a function of physical processes such as horizontal currents and vertical mixing with no additional biological behaviour that can influence the dispersal (Figure 3-3a). The other 8 dispersal scenarios are used to evaluate the influence that certain biological behaviours can have on the dispersal of particles. These scenarios are a subset of the 32 scenarios of Gary et al. (2020) and were chosen to demonstrate the sensitivity of connectivity estimates to a relatively wide range of larval behaviours, and which were also possible to implement in the dispersal model within the confines of available resources. A literature review was also undertaken to cross-check that the larval swimming speeds used by Gary et al. (2020) were relevant for VME indicator taxa (see Table 8-1 in the Annex). The specific details of the biological scenarios are as follows:

- Slow ascent to the surface (SSA; Figure 3-3b): particles are prescribed an upwards swimming velocity in addition to vertical mixing and vertical currents derived from the ocean model. A swimming velocity of 0.2 mm/s is used.
- Fast ascent to the surface (SFA; Figure 3-3c): this scenario is similar to SSA but particles are prescribed an upward swimming velocity of 1 mm/s.
- Drifting near the bottom (DNB; Figure 3-3d): particles are confined to drift near the seafloor.
- Drifting near surface (DNS; Figure 3-3e): particles that reach the surface through vertical mixing and vertical currents derived from the ocean model are confined to drift near the surface for the remainder of the simulation time.
- Drifting at release depth (DNR; Figure 3-3f): particles are confined to drift at the depth where they were originally released.
- Drifting in bottom model layer (DBL; Figure 3-3g): particles are confined to drift within the bottom terrain-following layer of the ocean model.
- Variable swimming with early descent to seafloor (VED; Figure 3-3h): particles are assigned an upwards swimming velocity of 1 mm/s for the first three days after their release followed by a downward velocity of 1 mm/s that is applied from day four onwards.
- Variable swimming with late descent to seafloor (VLD; Figure 3-3i): similar to VED, particles are assigned an upwards swimming velocity of 1 mm/s for the first three days after their release. Particles are then allowed to drift passively until day 42 at which point they are assigned a downward velocity of 1 mm/s.

For the scenarios in which vertical swimming is activated (SSA, SFA, VED and VLD), a prescribed 'swimming' velocity is added to the model-derived vertical velocity of each particle at each timestep. The upward swimming velocities of 1 mm/s and 0.2 mm/s applied in scenarios SFA and SSA, respectively, are consistent with the fast- and slow-ascent scenarios of Gary et al. (2020). Similarly, the larval ages at which downward swimming commences in scenarios VED and VLD match those used by Gary et al. (2020), while the prescribed downward swimming velocity is based on the maximum downward swimming speed reported in that study. In all scenarios, particles remain active near the seabed and continue to be advected by the simulated ocean currents.

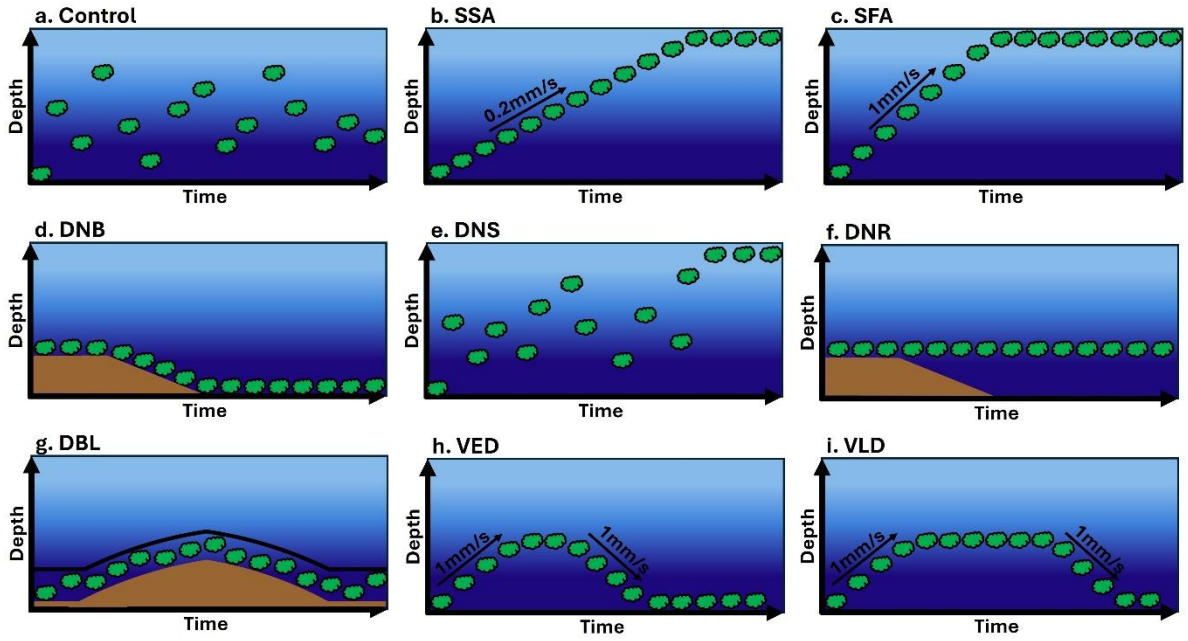

Figure 3-3 | Schematic representations of the different dispersal scenarios. a) Control, b) SSA: Slow ascent to the surface, c) SFA: Fast ascent to the surface, d) DNB: Drifting near the bottom, e) DNS: Drifting near the surface, f) DNR: Drifting at release depth, g) DBL: Drifting in bottom model layer, h) VED: Variable swimming with early descent to seafloor, i) VLD: Variable swimming with late descent to seafloor.

Analysis

All analyses were conducted separately for the different dispersal scenarios. The output from the 9 scenarios was evaluated for a single dispersal time duration, otherwise known as pelagic larval duration (PLD), of 30 days. The analysis consisted of estimating Lagrangian probability density functions (LPDFs), horizontal displacement, and quantifying the connectivity within- and between-bioregions for the different dispersal scenarios.

An instantaneous LPDF was calculated for each scenario to quantify the spatial distribution of particles at the end of the PLD. Particle positions from all seven bioregions were combined and binned onto a 50 km x 50 km grid. The number of particles within each grid cell was then normalized by the total number of particles included in the analysis, producing a probability distribution in which each grid cell represents the probability of finding a particle at that location at the specified PLD.

The connectivity between the seven bioregions was calculated as the proportion of released particles from each bioregion (N = 53,000) that reached another bioregion while the connectivity within a bioregion was calculated as the proportion of particles that remained within their release bioregions. The connectivity matrices together with the horizontal displacement, calculated as distance between each particle's release location and its position at the end of the PLD, are used to distinguish physical dispersal potential from realized population exchange.

4. Preliminary Results

Lagrangian Probability Density Functions (LPDFs)

The LPDFs of the different scenarios exhibit broadly similar spatial patterns, although several distinct differences in the spatial distributions of particles are apparent. In all scenarios, particle densities are highest within the bioregions and substantially lower outside these regions (Figure 4-1). Elevated particle densities consistently occur over prominent topographic features including Chatham Rise, Cambell Plateau, Challenger Plateau, and the Louisville Seamount Chain.

The LPDFs demonstrate that scenarios in which particles spend prolonged periods at the surface (SSA, SFA, DNS, and VLD; Figure 4-1 b, c, e and i) results in the greatest dispersal, whereas scenarios in which particles are transported near the seabed or within the deeper water column (Control, DNB, DNR, DBL, VED; Figure 4-1 a, d, f, g and h) exhibit the least dispersive behaviour.

LPDFs calculated for each individual bioregion under the different dispersal scenarios further demonstrates the contrasting dispersal patterns between the more and less dispersive scenarios. In the more dispersive scenarios, the LPDFs of the different bioregions indicate particle transport both within and beyond each of the seven bioregions (Figure 4-2). In contrast, the LPDFs of the different bioregions under the least dispersive scenarios show particle movement largely confined within individual bioregions, with only limited transport beyond their boundaries (Figure 4-3).

In addition, the LPDFs for the individual bioregions of the more dispersive scenarios also indicates that the limited eastward dispersal of particles from the coast of Australia into the Tasman Sea can largely be attributed to particles released within Bioregion 1 (Figure 4-2a) that are entrained into mesoscale eddies associated with the southward flowing East Australian Current. The more dispersive scenarios also exhibit eastward transport of particles from the Macquarie Ridge towards the Campbell Plateau (Figure 4-2g). This transport can largely be attributed to particles released from Bioregion 7 that become entrained in the eastward-flowing Antarctic Circumpolar Current and its associated frontal systems, particularly the Subantarctic Front, which skirts along the southern margin of the Campbell Plateau.

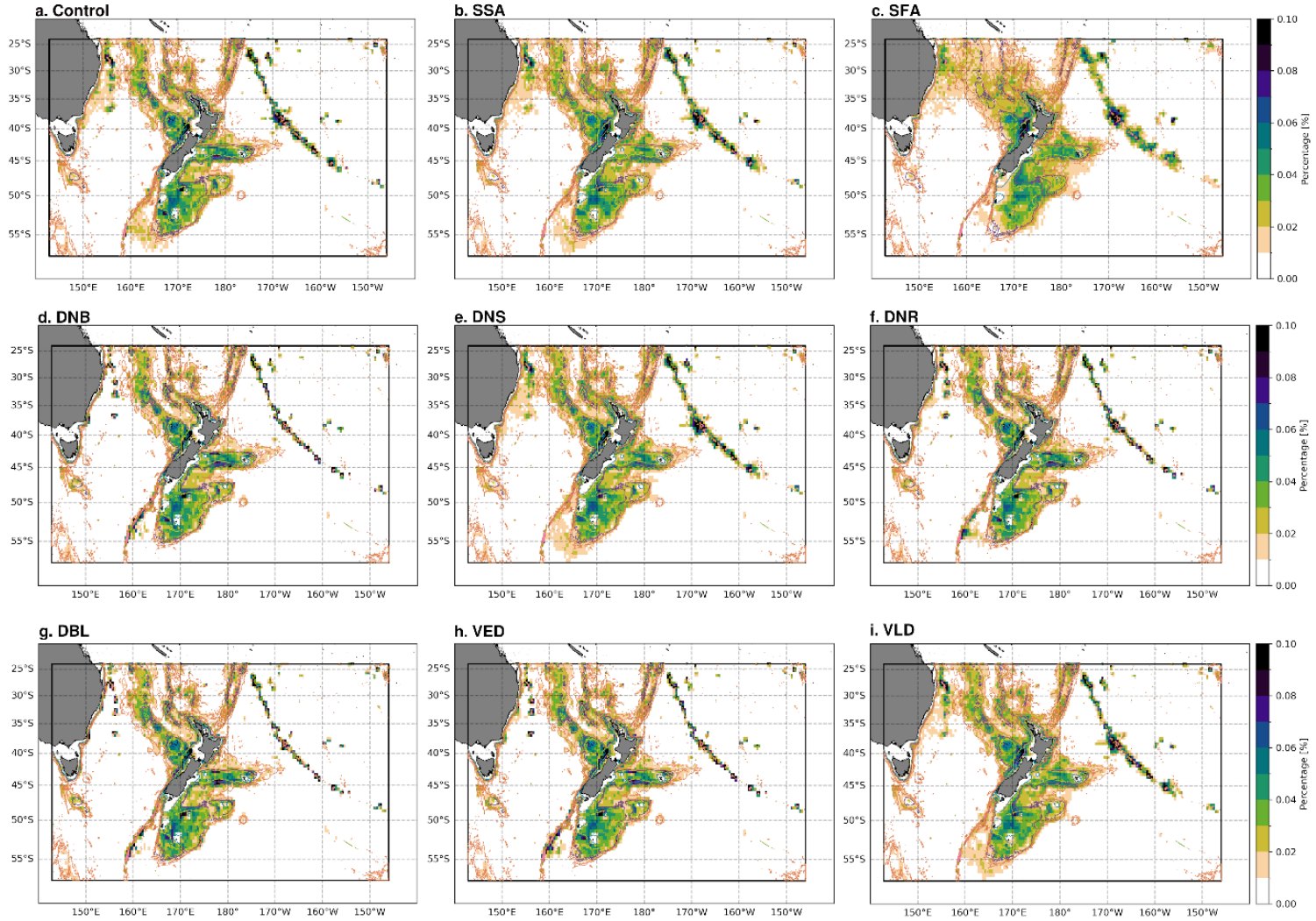

Figure 4-1 | Lagrangian Particle Density Functions (LPDFs) for the different dispersal scenarios calculated from the particle trajectories of all seven bioregions combined. The LPDFs were calculated on a 50 km x 50 km grid and are based on the spatial distribution of the particles at a PLD of 30 days. Darker colours indicate a higher probability of a particle being located in a particular grid cell, whereas lighter colours signify lower probabilities.

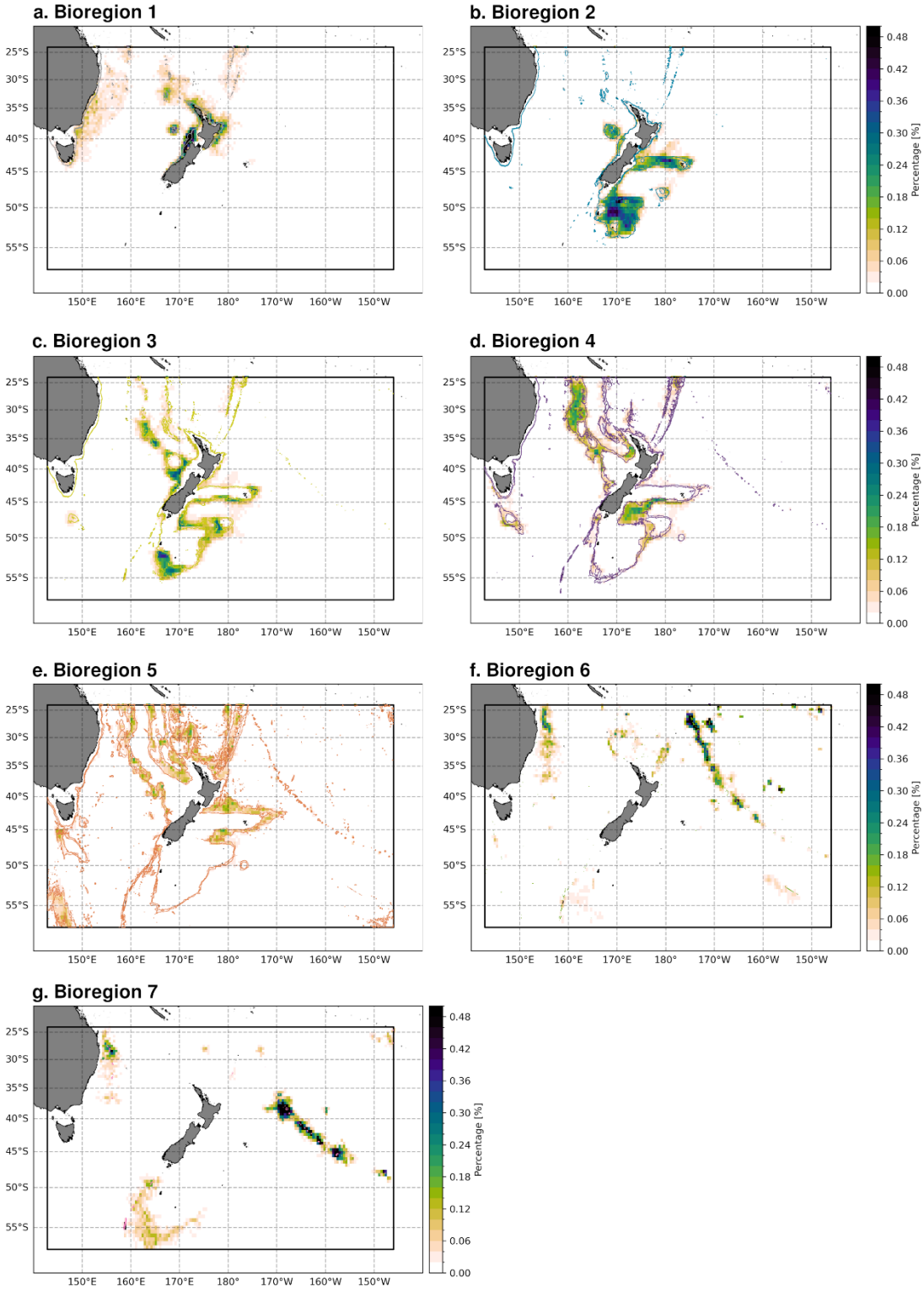

Figure 4-2 | Lagrangian Particle Density Functions (LPDFs) estimated for the different bioregion for the SSA dispersal scenario. The LPDFs were calculated on a 50 km x 50 km grid and are based on the spatial distribution of the particles at a PLD of 30 days. Darker colours indicate a higher probability of a particle being located in a particular grid cell, whereas lighter colours signify lower probabilities. The SFA, DNS and VLD scenarios have similar LPDFs for the individual bioregions (see Figure 8-1 to 8-3 in the Annex).

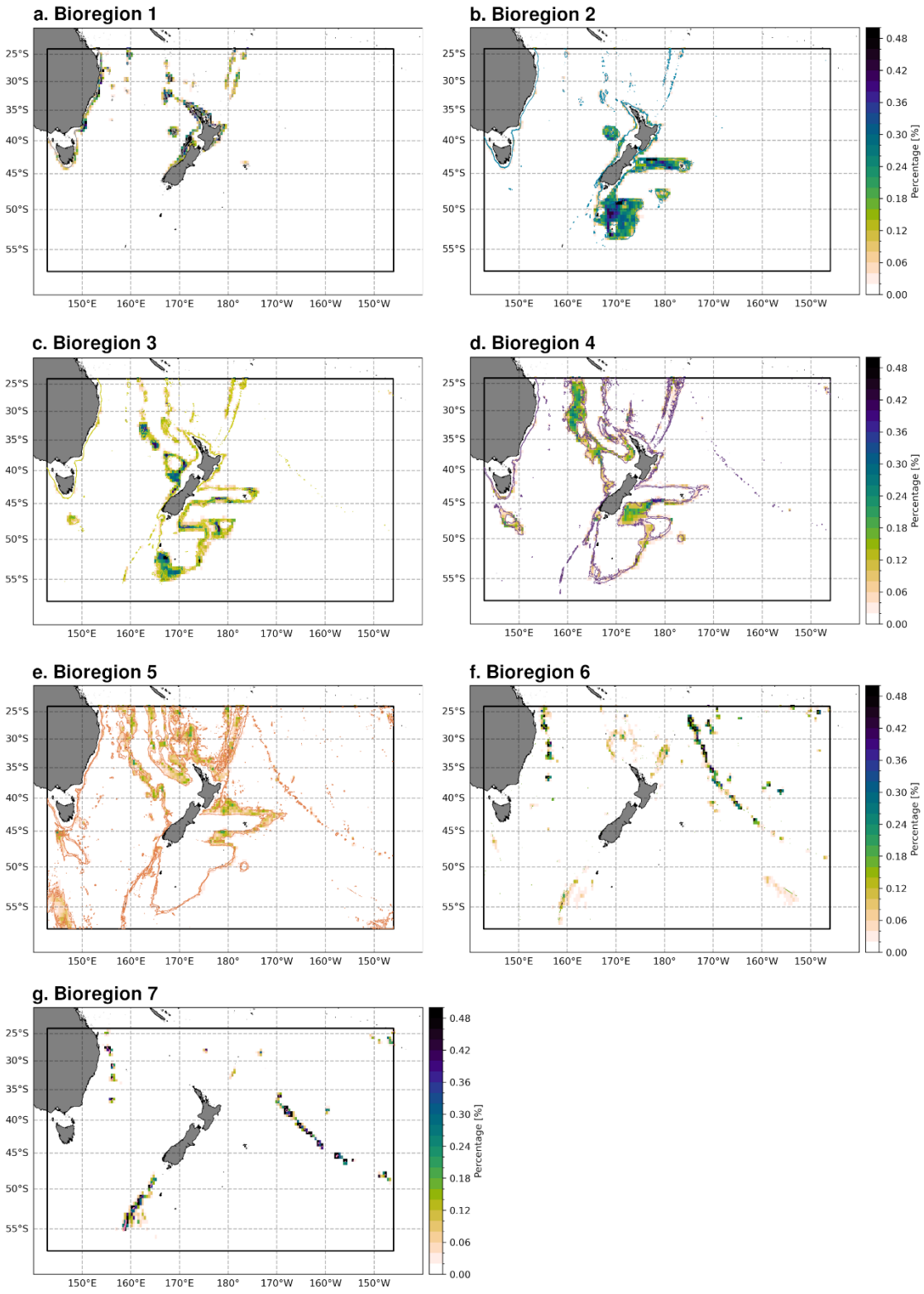

Figure 4-3 | Lagrangian Particle Density Functions (LPDFs) estimated for the different bioregion for the DNB dispersal scenario. The LPDFs were calculated on a 50 km x 50 km grid and are based on the spatial distribution of the particles at a PLD of 30 days. Darker colours indicate a higher probability of a particle being located in a particular grid cell, whereas lighter colours signify lower probabilities. The Control, DNR, DBL and VED scenarios have similar LPDFs for the individual bioregions (see Figures 8-4 to 8-7 in the Annex).

Connectivity matrices

The connectivity matrices for the different dispersal scenarios generally indicate higher levels of self-connectivity than connectivity among different bioregions (Figure 4-4). Together with the generally low horizontal displacement (Figure 4-5), suggests that particles are more likely to remain within their bioregion of origin than disperse to other bioregions.

The highest levels of self-connectivity across all bioregions are observed in scenarios where particles are transported near the seabed or within the water column (Control, DNB, DNR, DBL and VED). In contrast, scenarios in which particles spend prolonged periods at the surface (SSA, SFA, DNS and VLD) exhibit lower self-connectivity and greater connectivity among bioregions (Figure 4-4). This pattern is consistent with the horizontal displacement calculated for individual bioregions under the different dispersal scenarios, which shows that particles travel greater distances in the more dispersive scenarios (SSA, SFA, DNS, and VLD) than in the less dispersive scenarios (Control, DNB, DNR, DBL, VED; Figure 4-5). As expected, particles transported by stronger surface currents are advected farther over a given time period compared to particles advected by weaker bottom currents, increasing their likelihood of dispersing into neighbouring bioregions. Conversely, the lower horizontal displacement observed in the less dispersive scenarios, together with the LPDFs observed for the less dispersive scenarios, indicates that these particles remain closer to their release locations, resulting in more localized dispersal and higher levels of self-connectivity

The SFA scenario exhibits the lowest levels of self-connectivity across all the bioregions, while connectivity among bioregions remains moderate (Figure 4-4c). The reduced self-connectivity is likely a consequence of the rapid transport of particles away from their release locations by strong surface currents, as is reflected by the higher horizontal displacement observed across all bioregions under for this scenario (Figure 4-5c). The moderate levels of connectivity among bioregions in this scenario, on the other hand, suggest that although particles have an increased likelihood of reaching neighbouring bioregions, the PLD considered here is too short for particles released in this scenario to disperse to bioregions, or parts of bioregions, that are located farther from their bioregion of origin.

The connectivity matrices for the different scenarios generally indicate higher levels of self-connectivity within Bioregions 2-5 (Figure 4-4). Bioregion 1, which exhibits the greatest mean horizontal displacement in most of the dispersal scenarios, is the most well-connected bioregion, contributing more than 5% of its particles to each of Bioregions 2-5 across all nine scenarios. In contrast, in all of the dispersal scenarios, Bioregions 6 and 7 receives less than 2% of the particles released from other bioregions, but at least 10% of the particles released from these two bioregions are transported into Bioregion 5, indicating a predominantly one-way pattern of connectivity.

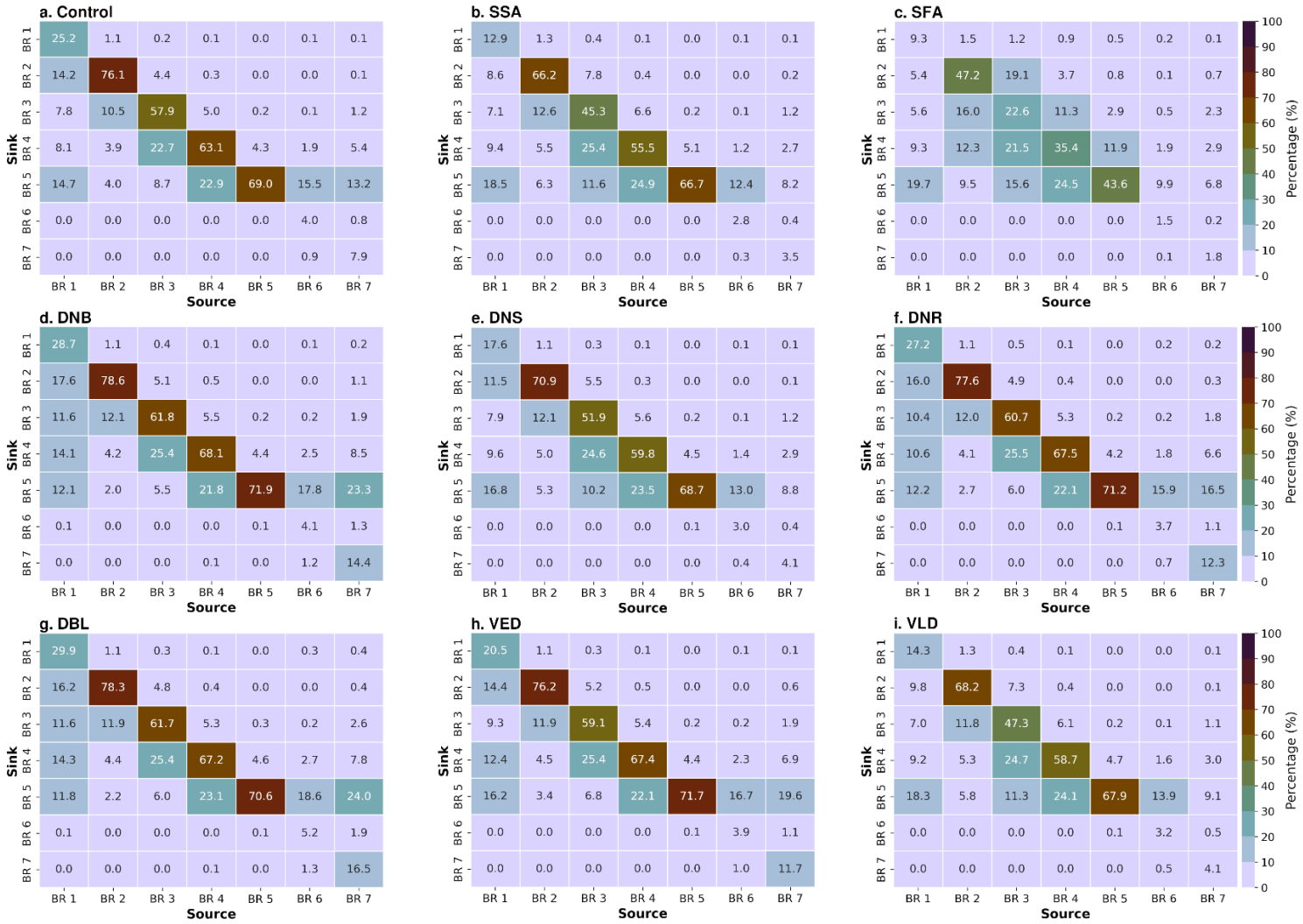

Figure 4-4 | Connectivity between the seven bioregions (BR-1 to BR-7) for the different dispersal scenarios for a PLD of 30 days showing the percentage of virtual larvae released in one bioregion (x axis) that are transported (y axis) into the same or another bioregion. The exact percentage values are indicated by both the colour bar and the text in each cell.

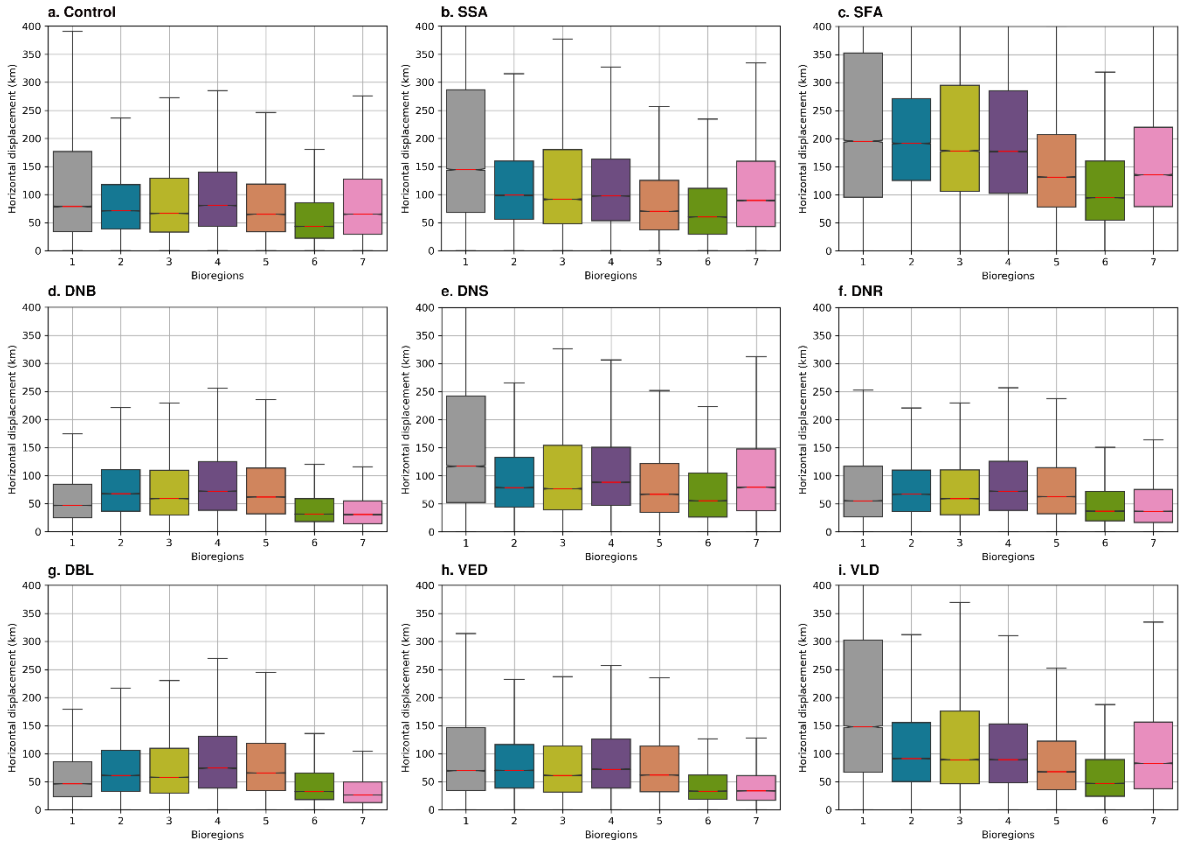

Figure 4-5 | Horizontal displacement for the individual bioregions under the nine different dispersal scenarios. The horizontal displacement is calculated as the distance (in km) between the start location of each particle and its location at the end of a PLD of 30 days.

5. Discussion

The dispersal modelling presented here improves upon the modelling previously used as one of several approaches to validate the bioregionalization of VME indicator taxa (SC13-DW10) in two ways. First, the dispersal modelling presented here is driven by ocean currents from a higher-resolution ocean model that is capable of resolving baroclinic instabilities and the resulting mesoscale eddy field. Second, it incorporates biologically realistic larval behaviours, such as vertical swimming and depth of dispersal, which have been shown to substantially influence larval dispersal pathways and connectivity patterns (Gary et al. 2020; McVeigh et al. 2017).

The preliminary results from the nine dispersal scenarios indicate that the biologically realistic larval behaviours incorporated into the dispersal modelling has a significant impact on dispersal patterns and connectivity. In particular, particles advected near the surface for extended periods exhibit greater dispersal than particles that remain deeper in the water column or close to the seabed. Accordingly, these scenarios are characterised by lower self-connectivity and greater connectivity among bioregions. Particles drifting near the surface are exposed to stronger and more variable currents, enabling them to travel greater distances over a given time period compared to particles at depth. This increased transport enhances the likelihood of dispersal between bioregions and, consequently, increases connectivity among them. Particles drifting deeper in the water column experience weaker and more stable flow conditions, resulting in more limited dispersal and higher self-connectivity.

The difference in connectivity noted between Bioregion 1 and Bioregions 6-7 likely reflects the contrasting oceanographic settings of these bioregions. Much of Bioregion 1 lies along the continental shelves of Australia and New Zealand, where stronger shelf currents enhance particle transport. In contrast, Bioregions 6 and 7 are predominantly associated with offshore ridges and seamount chains in the open ocean, where weaker currents result in reduced particle displacement. The relatively small spatial extent of the individual seamounts that comprise Bioregions 6 and 7, relative to the horizontal resolution of the ocean model used to drive the dispersal simulations, means that the circulation associated with the seamounts is not fully resolved by the large-scale regional model. As a result, fine-scale hydrodynamic processes that may influence local particle retention and dispersal are likely underrepresented.

The next phase of this work will focus on developing a higher resolution ocean model for part of the Louisville Seamount Chain to improve the dispersal modelling within Bioregions 6 and 7. In parallel, the analyses will be refined to examine dispersal patterns in more detail, with a particular emphasis on particle transport from different parts of the same bioregion. The analyses presented here will also be extended evaluate a broader range of PLDs, while incorporating biological constraints on survival, such as depth thresholds. In addition, a targeted literature review will be conducted to identify the larval behaviour scenarios that best reflect the ecology VME indicator taxa. Together, these refinements will improve the biological realism of the dispersal modelling and ensure that its outputs are more relevant to VME indicator taxa.

6. Recommendations

It is recommended that the Scientific Committee:

- **Notes:**
  - that the particle tracking approach developed to contribute to validation of the South Pacific VME bioregionalisation has been improved by incorporating a higher-resolution regional model and the impact of biological behaviour.
  - that the approach presented can resolve baroclinic instabilities and the resulting mesoscale eddy field.
  - that the approach incorporates biologically realistic larval behaviours, such as vertical swimming and depth of dispersal, which have been shown to substantially influence larval dispersal pathways and connectivity patterns.
- **Agrees:**
  - that, while results are still preliminary, incorporating behaviour and finer scale processes has improved upon the modelling previously used as one of several approaches to validate the bioregionalization of VME indicator taxa.
  - that the particle tracking model should be progressed to include a higher resolution ocean model for part of the Louisville Seamount Chain to resolve fine scale dispersal patterns within Bioregions 6 and 7 in this region.
  - that the dispersal patterns should be examined in more detail, with a particular emphasis on particle transport from disparate and fragmented areas, within same bioregion.

- that the analysis should evaluate a broader range of PLDs, while incorporating biological realism in constraints on survival, and that a broader literature review be conducted to identify the larval behaviour scenarios that best reflect the ecology VME indicator taxa in the South Pacific.

7. Acknowledgements

Funding for this study was provided by Fisheries New Zealand, Ministry for Primary Industries under project SPR2023-01. The authors acknowledge the useful input received from members of the South Pacific Working Group (SPACWG).

8. References

Abdul Wahab, M.A., de Nys, R., Webster, N., Whalan, S. (2014) Larval behaviours and their contribution to the distribution of the intertidal coral reef sponge *Carteriospongia foliascens*. *PLoS ONE*, 9(5), e98181. doi:10.1371/journal.pone.0098181

Brooke, S., Young, C.M. (2005) Embryogenesis and larval biology of the ahermatypic scleractinian *Oculina varicosa*. *Marine Biology*, 146, 665–675. doi:10.1007/s00227-004-1481-9

Chia, F-S., Buckland-Nicks, J., Young, C.M. (1984) Locomotion of marine invertebrate larvae: a review. *Canadian Journal of Zoology*, 62, 1205–1222. doi:10.1139/z84-176

Costello, M. J., P. Tsai, P. S. Wong, A. K. L. Cheung, Z. Basher, and C. Chaudhary. (2017). Marine biogeographic realms and species endemicity. Nature Communications 8:1057.

Cowen, R. K., and S. Sponaugle. (2009). Larval dispersal and marine population connectivity. Annu. Rev. Mar. Sci. 1:443-466.

Dagestad, K. F., J. Röhrs, Ø. Breivik, and B. Ådlandsvik. (2018). OpenDrift v1.0: a generic framework for trajectory modelling. Geosci. Model Dev. 11:1405-1420.

Dee, D.P., S. Uppala, A. J. Simmons, P. Berrisford, P. Poli, S. Kobayashi, U. Andrae, M. A. Balmaseda, G. Balsamo, D. P. Bauer, P. Bechtold. (2011). The ERA-Interim reanalysis: Configuration and performance of the data assimilation system. Q. J. R. Meteorol. Soc. 137:553-597.

Fagerström, V., Broström, G., Larsson, A.I. (2022) Turbulence affects larval vertical swimming in the cold-water coral *Lophelia pertusa*. *Frontiers in Marine Science*, 9, 1062884. doi:10.3389/fmars.2022.1062884

Gary, S.F., A. D. Fox, A. Biastoch, J. M. Roberts, S. A. Cunningham. (2020). Larval behaviour, dispersal and population connectivity in the deep sea. Scientific Reports 10:10675

Hallberg, R. (2013). Using a resolution function to regulate parameterizations of oceanic mesoscale eddy effects. Ocean Modelling 72:92-103

Hata, T., Madin, J.S., Cumbo, V.R., Denny, M., Figueiredo, J., Harii, S., Thomas, C.J., Baird, A.H., (2017). Coral larvae are poor swimmers and require fine-scale reef structure to settle. *Scientific reports*, *7*(1), p.2249.

Jean-Michel, L., G. Eric, B.-B. Romain, G. Gilles, M. Angélique, D. Marie, B. Clément, H. Mathieu, L. G. Olivier, R. Charly, C. Tony, T. Charles-Emmanuel, G. Florent, R. Giovanni, B. Mounir, D. Yann, L. T. Pierre-Yves. (2021). The Copernicus Global 1/12° Oceanic and Sea Ice GLORYS12 Reanalysis. Frontiers in Earth Science Volume 9 - 2021.

Klanten, O. S., M. Gall, S. S. Barbosa, M. W. Hart, C. C. Keever, J. B. Puritz, J. Harantio, R. J. Toonen, P. Selvakumaraswamy, R. K. Grosberg. (2023). Population connectivity across east Australia's bioregions and larval duration of the range-extending sea star Meridiastra calcar. Aquatic Conservation: Marine and Freshwater Ecosystems 33:1061-1078.

Lanna, E., Riesgo, A. (2020) Sponge larvae do not swim that fast: a reply to Montgomery et al. (2019). *Journal of the Marine Biological Association of the United Kingdom*, 100(1), 181–183. doi:10.1017/S0025315419000870

Le Sommer, J., E. P. Chassignet, A. J. Wallcraft. (2018). Ocean circulation modeling for operations oceanography: Current status and future challenges. New Frontiers in operational oceanography.

Limer, B.D., Payne, O., Brancato, A., Mitchell, M., Abu-Kubie, C., Figueiredo, J., Holstein, D.M. (2024) Life history and early ontogeny determine vertical swimming behaviors in the larvae of Caribbean corals. *Journal of Experimental Marine Biology and Ecology*, 578, 152035. doi:10.1016/j.jembe.2024.152035

McVeigh, D.M., Eggleston, D.B., Todd, A.C., Young, C.M., He, R. (2017) The influence of larval migration and dispersal depth on potential larval trajectories of a deep-sea bivalve. *Deep Sea Research Part I*, 127, 57–64. doi:10.1016/j.dsr.2017.08.002

Michie, C., Lundquist, C.J., Lavery, S.D., Della Penna A. (2024) Spatial and temporal variation in the predicted dispersal of marine larvae around coastal Aotearoa New Zealand. Front. Mar. Sci. 10:1292081. doi:10.3389/fmars.2023.1292081

Montgomery, E.M., Hamel, J-F., Mercier, A. (2019) Larval nutritional mode and swimming behaviour in ciliated marine larvae. *Journal of the Marine Biological Association of the United Kingdom*, 99(5), 1027–1032. doi:10.1017/S0025315418001091

Strömberg, S.M.,Larsson, A.I. (2017) Larval behavior and longevity in the cold-water coral *Lophelia pertusa* indicate potential for long distance dispersal. *Frontiers in Marine Science*, 4, 411. doi:10.3389/fmars.2017.00411

Shchepetkin, A. F., and J. C. McWilliams. (2005). The Regional Ocean Modeling System (ROMS): a split-explicit, free-surface, topography-following-coordinate oceanic model. Ocean Modelling 9: 347-404

Stephenson, F., A. A. Rowden, J. Tablada, K. Tunley, T. Brough, C. J. Lundquist, D. A. Bowden, and S. Geange. (2023). A seafloor bioregionalisation for New Zealand. Ocean & Coastal Management 242:106688.

Stephenson, F., J. Tablada, A. A. Rowden, R. Bulmer, D. A. Bowden, S. W. Geange. (2024). Independent statistical validation of the New Zealand Seafloor Community Classification. Aquatic Conservation: Marine and Freshwater Ecosystems 34:e4114.

Woolley, S. N. C., S. D. Foster, N. J. Bax, J. C. Currie, D. C. Dunn, C. Hansen, N. Hill, T. D. O'Hara, O. Ovaskainen, R. Sayre, J. P. Vanhatalo, and P. K. Dunstan. (2019). Bioregions in Marine Environments: Combining Biological and Environmental Data for Management and Scientific Understanding. BioScience 70:48-59.

Zúñiga Mouret, R., Hourdez, S., Curran, M., DiBenedetto, M.H., Mills, S.W., Vetriani, C., Arellano, S.M., Weston, J.N.J., Dykman, L.N., Best, A.C., Pires, A., Mullineaux, L.S. (2025) Pressurized plankton observatory offers a new window into deep-sea larval behavior. *Limnology and Oceanography: Methods*, 23, 638–651. doi:10.1002/lom3.10708

9. Annex

Table 9-1 Summary of information derived from a literature review of larval behaviours.

Reference	Taxon	Horizontal (mm s^{-1})	Vertical (mm s^{-1})	Behaviour
Fagerström et al. (2022)	*Lophelia pertusa*	0.23–0.5	0.3–0.5	Strong upward swimming, 3–5 weeks
Strömberg & Larsson (2017)	*Lophelia pertusa*	–	0.5–0.7	Upward early; bottom-probing from week 3
Hata et al. (2017)	Scleractinia (meta-analysis)	1.57–2.73	1.66–4.79	Poor swimmers; can't overcome currents
Lanna & Riesgo (2020)	Porifera	5.11 ± 9.21	–	–
Montgomery et al. (2019)	Bryozoa / Echinodermata / Porifera	0.04–45 (range across taxa)	–	–
Abdul Wahab et al. (2014)	Sponge (*Carteriospongia*)	2.2–4.3	2.2–4.3	Down at release; up at night; benthic by 34h
McVeigh et al. (2017)	Mollusc (model)	–	0.2–2	Upwards week 1–2; drifts ~375d; down near settlement
Brooke & Young (2005)	*Oculina varicosa*	0.2–0.5	0.2–0.5	Up & shallow early; later down, light-avoiding, probing
Limer et al. (2024)	Caribbean corals	3.24–8.51	3.25–8.89	Brooders: down early; spawners: up, prolonged dispersal
Zúñiga Mouret et al. (2025)	Gastropods/copepods	–	0.3–1.5	Speed rises with biofilm; fine-scale cues, not clear direction
Chia et al. (1984)	Demosponge/Scleractinia/Gorgonian/Bryozoa	~2–10	1.6–2.7	Basis for Michie et al. (2024) model (see PLD literature review therein): up 0.2 early, down −0.25 post-settlement age

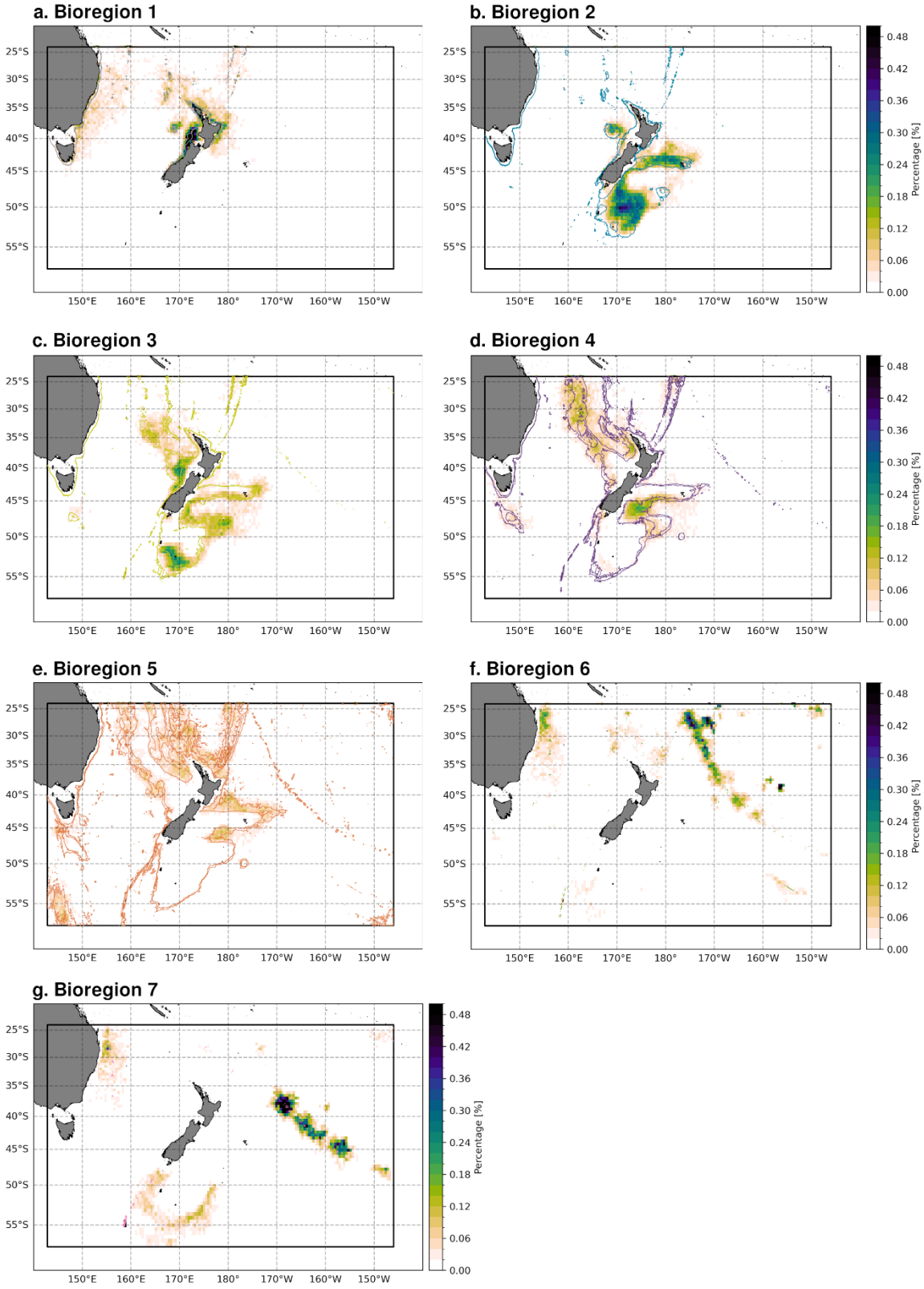

Figure 8-1 | Lagrangian Particle Density Functions (LPDFs) estimated for the different bioregion for the SFA dispersal scenario. The LPDFs were calculated on a 50 km x 50 km grid and are based on the spatial distribution of the particles at a PLD of 30 days. Darker colours indicate a higher probability of a particle being located in a particular grid cell, whereas lighter colours signify lower probabilities.

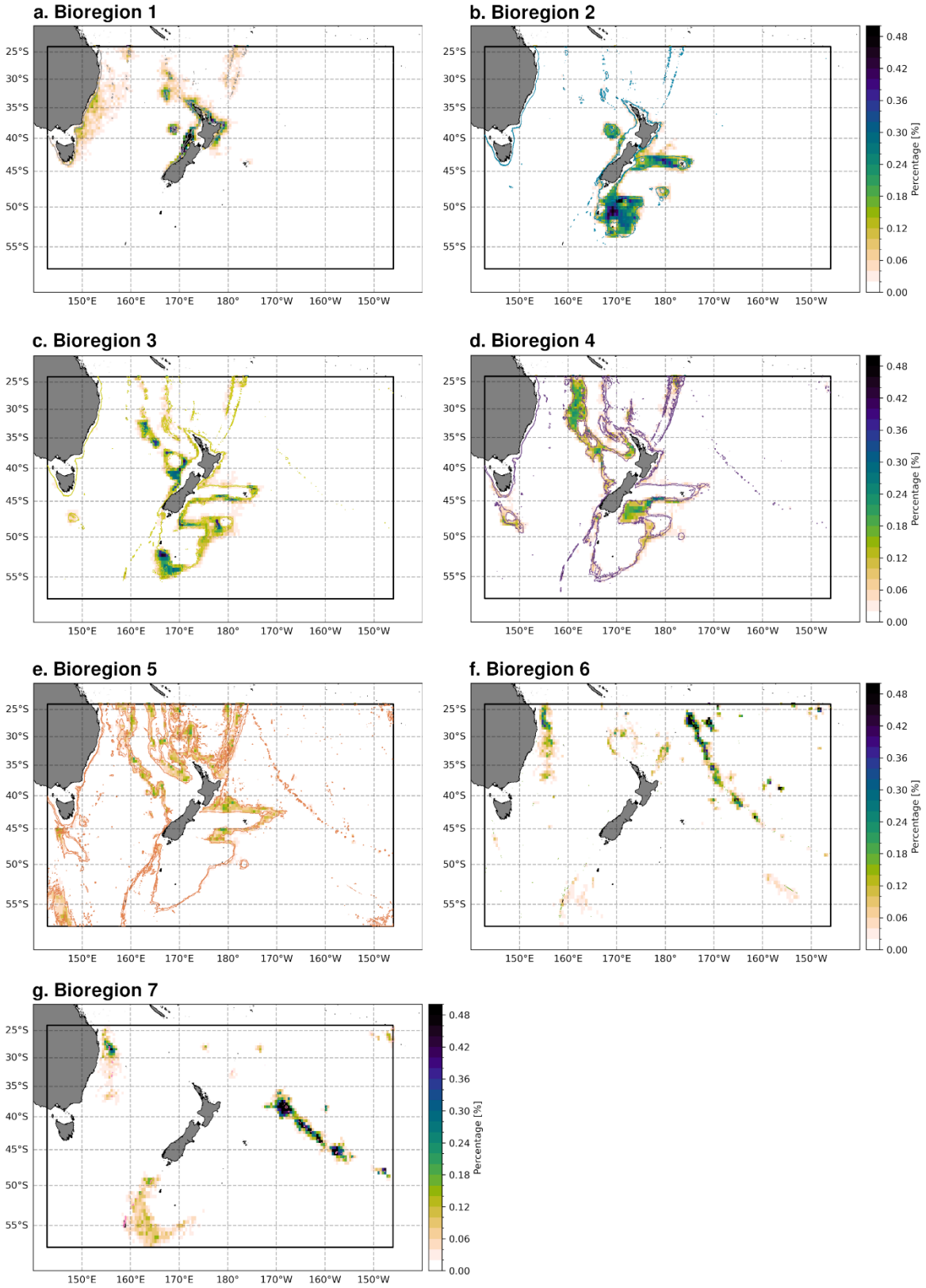

Figure 8-2 | Lagrangian Particle Density Functions (LPDFs) estimated for the different bioregion for the DNS dispersal scenario. The LPDFs were calculated on a 50 km x 50 km grid and are based on the spatial distribution of the particles at a PLD of 30 days. Darker colours indicate a higher probability of a particle being located in a particular grid cell, whereas lighter colours signify lower probabilities.

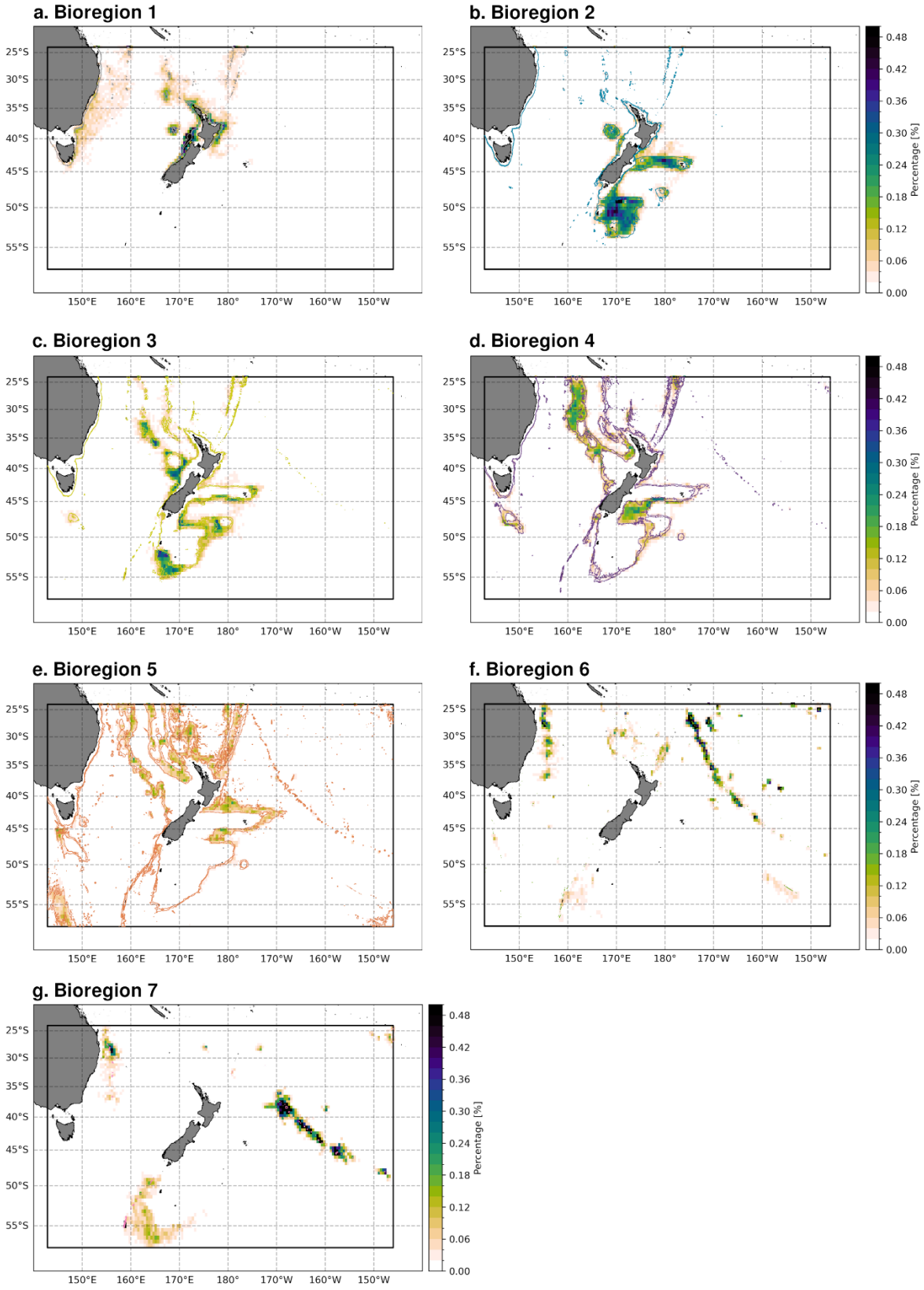

Figure 8-3 | Lagrangian Particle Density Functions (LPDFs) estimated for the different bioregion for the VLD dispersal scenario. The LPDFs were calculated on a 50 km x 50 km grid and are based on the spatial distribution of the particles at a PLD of 30 days. Darker colours indicate a higher probability of a particle being located in a particular grid cell, whereas lighter colours signify lower probabilities.

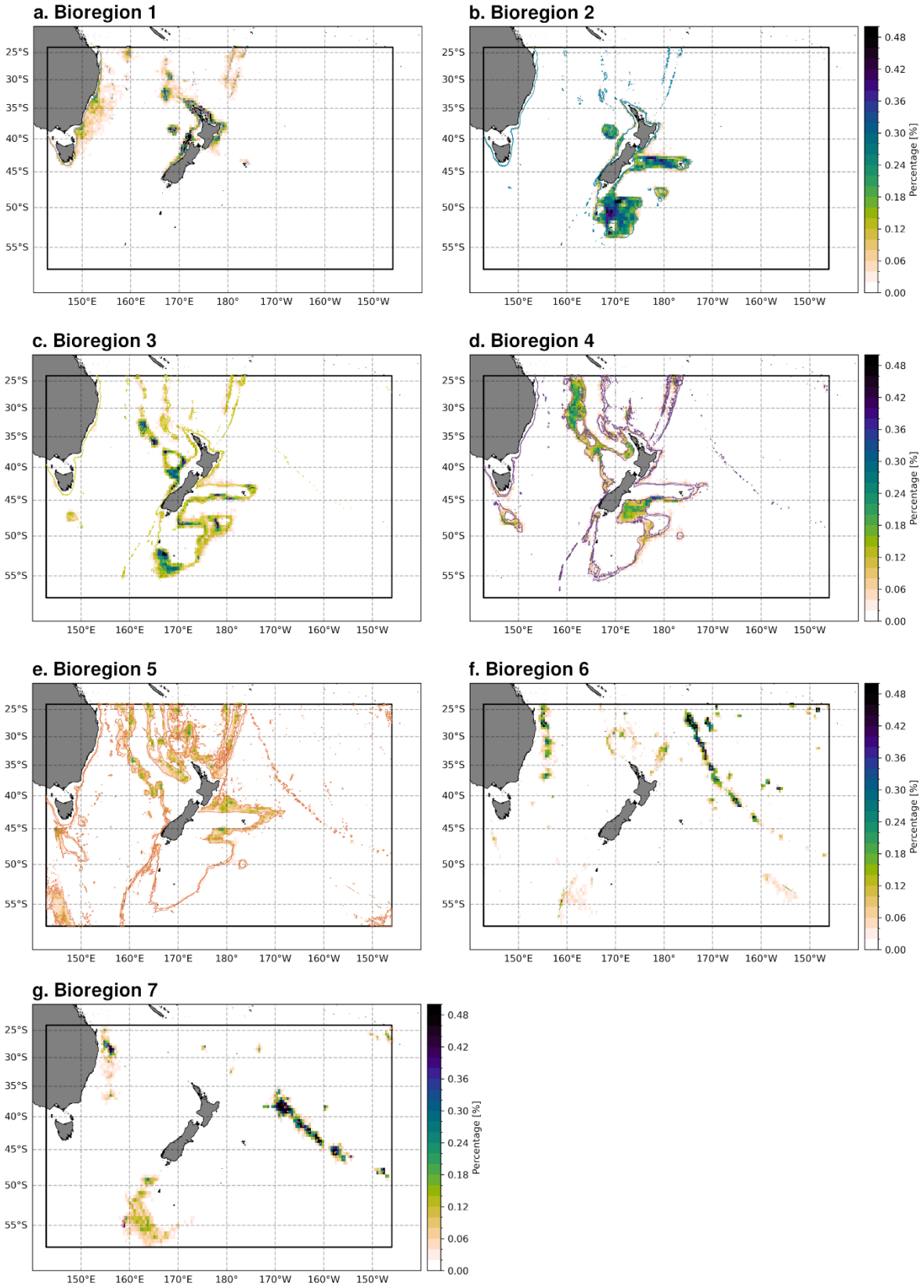

Figure 8-4 | Lagrangian Particle Density Functions (LPDFs) estimated for the different bioregion for the Control dispersal scenario. The LPDFs were calculated on a 50 km x 50 km grid and are based on the spatial distribution of the particles at a PLD of 30 days. Darker colours indicate a higher probability of a particle being located in a particular grid cell, whereas lighter colours signify lower probabilities.

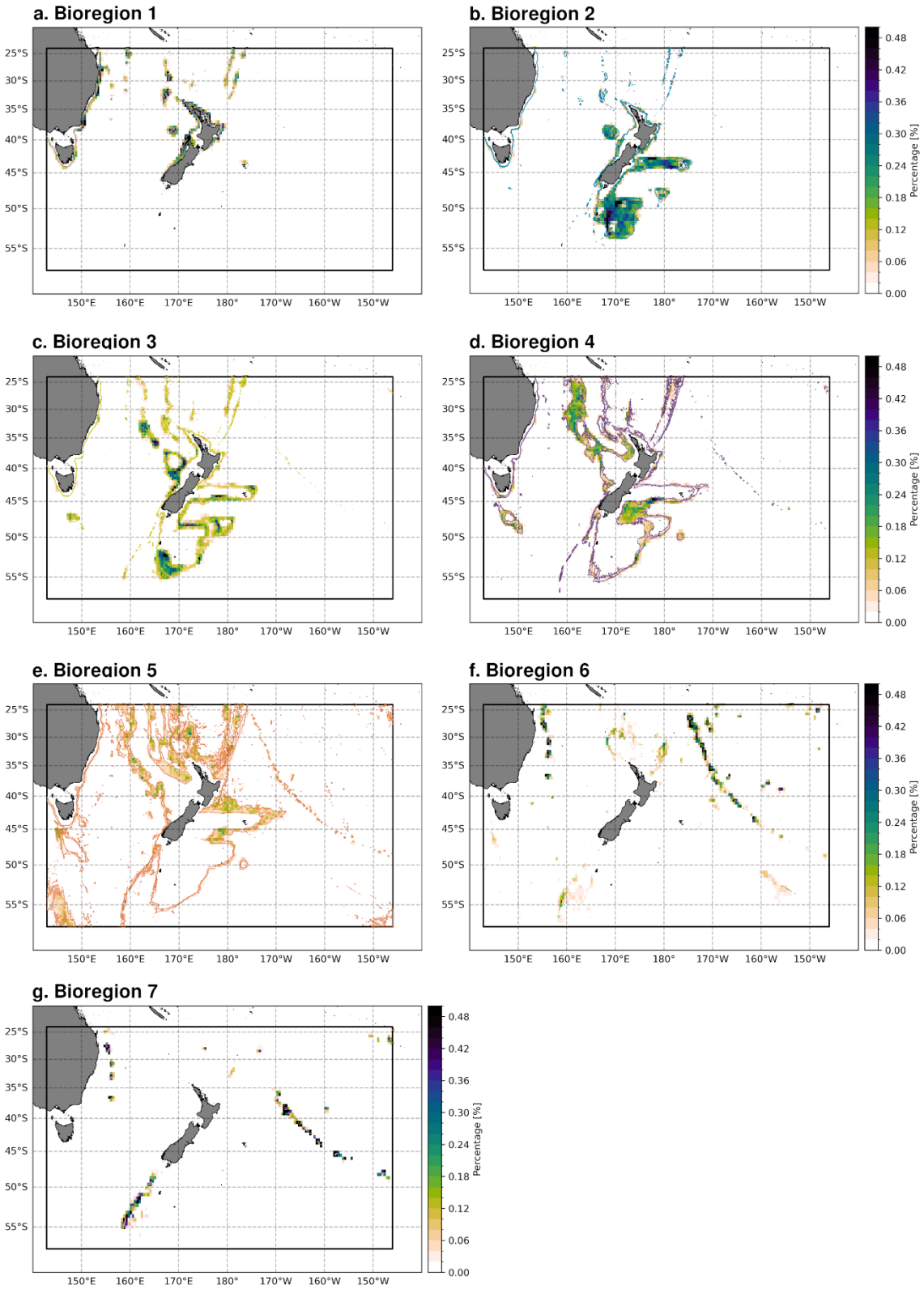

Figure 8-5 | Lagrangian Particle Density Functions (LPDFs) estimated for the different bioregion for the DBL dispersal scenario. The LPDFs were calculated on a 50 km x 50 km grid and are based on the spatial distribution of the particles at a PLD of 30 days. Darker colours indicate a higher probability of a particle being located in a particular grid cell, whereas lighter colours signify lower probabilities.

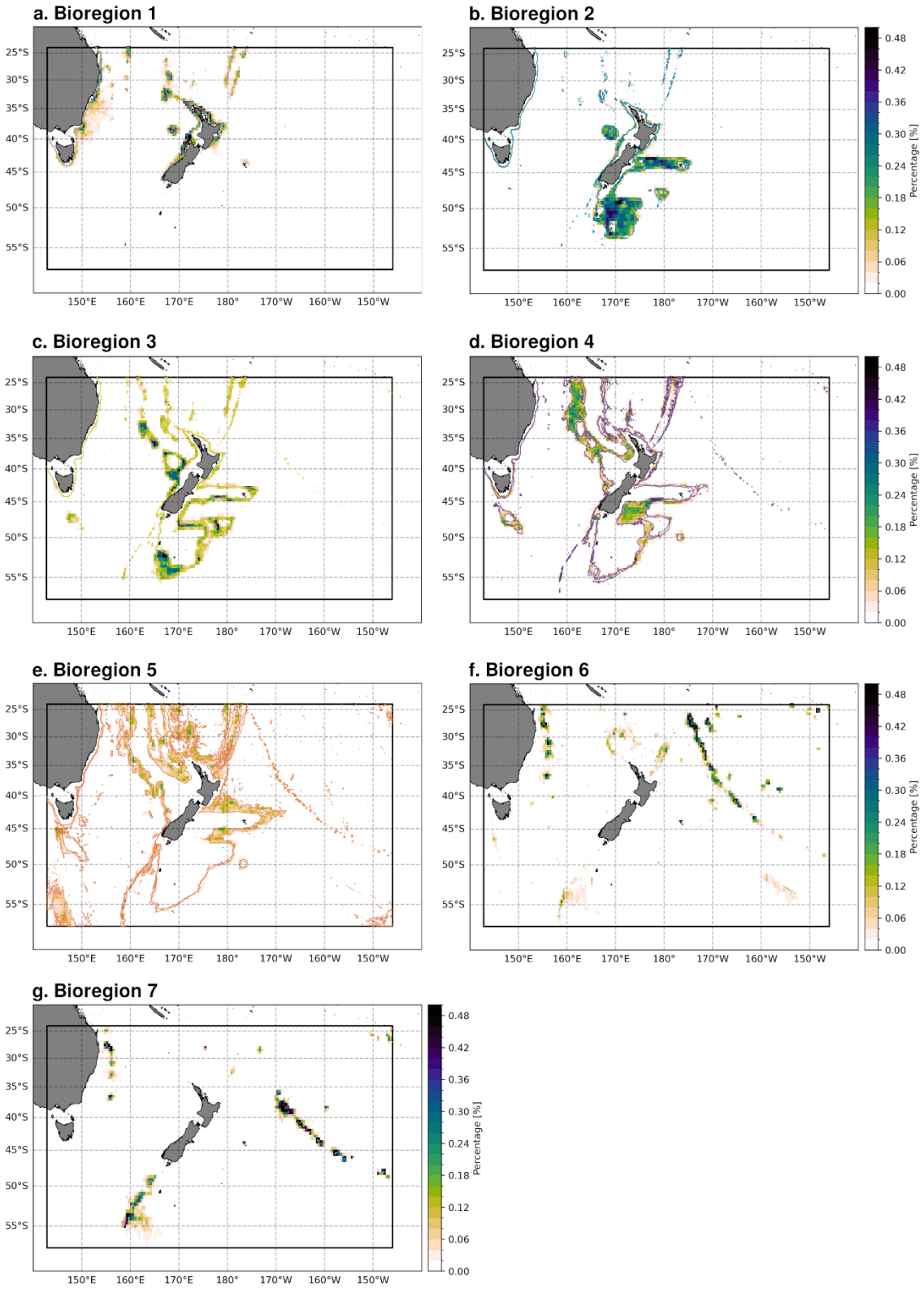

Figure 8-6 | Lagrangian Particle Density Functions (LPDFs) estimated for the different bioregion for the DNR dispersal scenario. The LPDFs were calculated on a 50 km x 50 km grid and are based on the spatial distribution of the particles at a PLD of 30 days. Darker colours indicate a higher probability of a particle being located in a particular grid cell, whereas lighter colours signify lower probabilities.

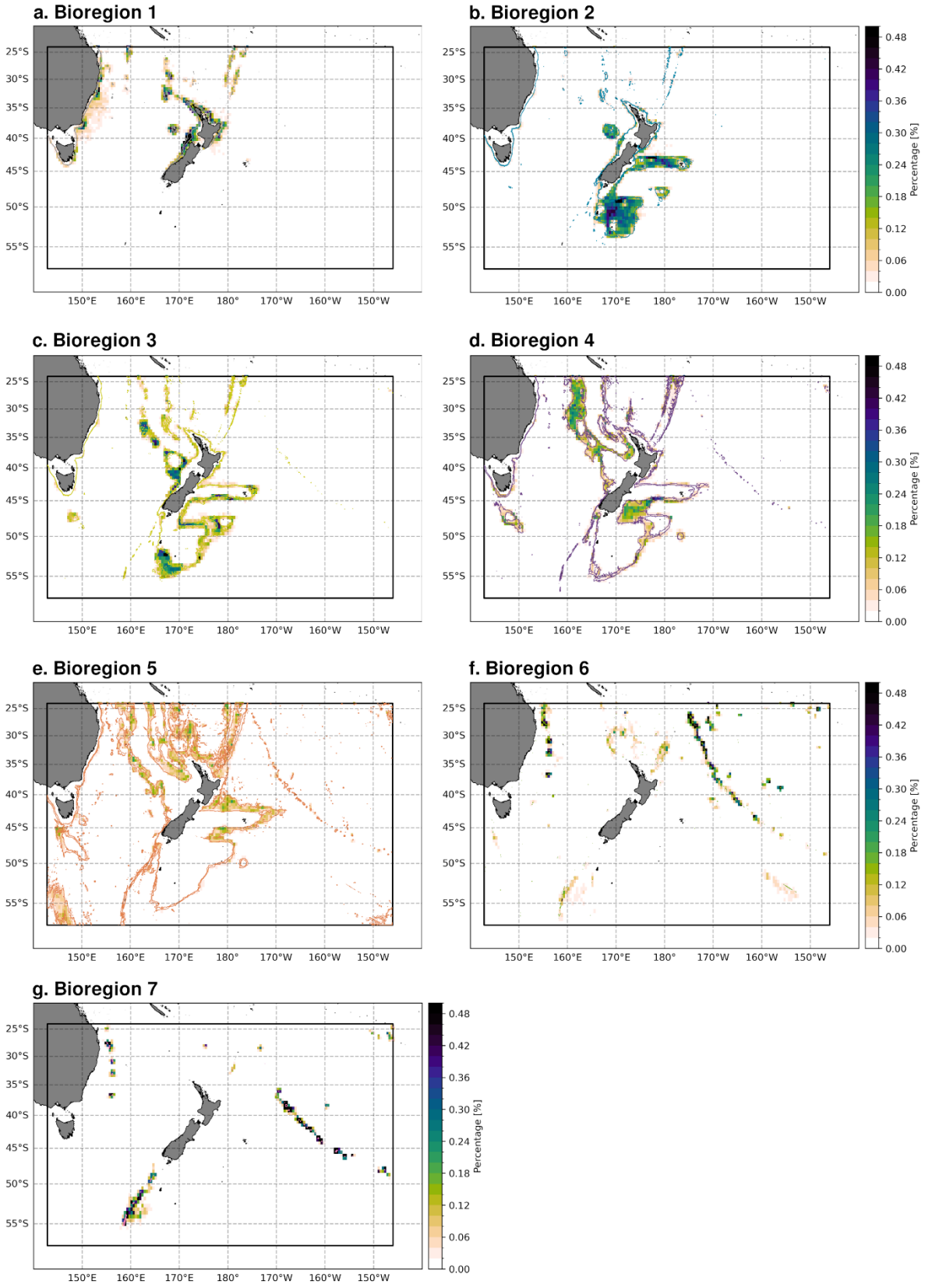

Figure 8-7 | Lagrangian Particle Density Functions (LPDFs) estimated for the different bioregion for the VED dispersal scenario. The LPDFs were calculated on a 50 km x 50 km grid and are based on the spatial distribution of the particles at a PLD of 30 days. Darker colours indicate a higher probability of a particle being located in a particular grid cell, whereas lighter colours signify lower probabilities.